Composite solitons and two-pulse generation in passively mode-locked lasers modeled by the complex quintic Swift-Hohenberg equation

J. M. Soto-Crespo*
Instituto de Óptica, CSIC, Serrano 121, 28006 Madrid, Spain

Nail Akhmediev
Optical Sciences Centre, Research School of Physical Sciences and Engineering, The Australian National University, Canberra, Australian Capital Territory 0200, Australia

(Received 9 August 2002; published 18 December 2002)

The complex quintic Swift-Hohenberg equation (CSHE) is a model for describing pulse generation in mode-locked lasers with fast saturable absorbers and a complicated spectral response. Using numerical simulations, we study the single- and two-soliton solutions of the $(1+1)$-dimensional complex quintic Swift-Hohenberg equations. We have found that several types of stationary and moving composite solitons of this equation are generally stable and have a wider range of existence than for those of the complex quintic Ginzburg-Landau equation. We have also found that the CSHE has a wider variety of localized solutions. In particular, there are three types of stable soliton pairs with π and $\pi/2$ phase difference and three different fixed separations between the pulses. Different types of soliton pairs can be generated by changing the parameter corresponding to the nonlinear gain (ϵ).

DOI: 10.1103/PhysRevE.66.066610 PACS number(s): 42.65.Tg, 42.65.Sf, 47.20.Ky, 47.52.+j

I. INTRODUCTION

Passive mode locking allows the generation of self-shaped ultrashort pulses in a laser system [1]. It has been explained in a number of works that the pulses generated by mode-locked lasers are solitons [2,3]. Fiber lasers are potentially useful in optical communications [4]. Solid state lasers produce the shortest pulses, down to a few femtoseconds long [5,6]. Apart from all its important applications, the mode-locked laser is an interesting object for studies, as it is a nonlinear system that can have a very rich dynamics. Short-pulse lasers are susceptible to various instabilities, period doubling [7,8], pulsating behavior [9], various routes to chaos [10–12], explosive instabilities [13], and switching to double-pulse generation [14–16]. Another interesting feature that can potentially have a variety of applications, is that the generated pulses can have complicated symmetric and asymmetric profiles [17] which are also solitons. Thus far, these have not been observed experimentally. One of the aims of this work is a proposal to facilitate their observation, as well as the observation of multisoliton solutions.

The convenience of using a single master equation for describing complicated phenomena such as ultrashort-pulse generation in laser systems is unquestioned [18]. This can be done in certain limits that are valid for a variety of laser systems. In the case of a laser with a fast saturable absorber, the original equations can be reduced to a single complex Ginzburg-Landau equation (CGLE). It has been realized [19] that the simplest case of the cubic CGLE is not adequate for a realistic description of any actual system. The quintic nonlinearity is essential for ensuring the stability of solitonlike pulses [19]. Another restriction is that spectral filtering in the CGLE model is limited to a second-order term and can describe only a spectral response with a single maximum. In an experiment, the gain spectrum is usually wide and might have several maxima. It is clear that higher-order filtering terms are essential for both making the model more realistic, and for describing more involved pulse generation effects. The addition of a fourth-order spectral filtering term into the CGLE model transforms it into the complex Swift-Hohenberg equation (CSHE).

This equation has already been considered in relation to spatial structures in large-aspect lasers [20]. It is also used for describing instabilities and pattern formation phenomena in cases of Rayleigh-Bénard convection [21] and in oscillating chemical reactions [22]. The CSHE is also important in describing pulse generation processes in passively mode-locked lasers with fast saturable absorbers. The higher-order derivatives are then responsible for higher-order dispersion in the cavity, as well as complicated spectral filtering. The role of higher-order dispersion effects in soliton formation has been studied before in Refs. [23–26]. Our task here is to study dissipative effects, namely, the role of higher-order terms in spectral filtering. As far as we know, this has not been done before.

More specifically, our aim here is to compare the solutions of the CSHE model with those appearing in the CGLE model of a passively mode-locked laser. The two models differ in the spectral filtering effect. We may expect that pulse generation effects in the case of the CSHE model would be similar to those in the CGLE model. This is true, to some extent, as we have found in our numerical simulations. At the same time some additional effects also appear.

The variety of solutions appearing in the CSHE model of a laser is enormous. Any attempt to classify them in one work would fail. This means that we have to analyze some limited range of solutions, starting from the known limit of the CGL equation. The difficulty in doing this with a fourth-

*Electronic address: iodsc09@io.cfmac.csic.es

order derivative in the equation is that this term cannot be considered as a perturbation with a small coefficient in front of it. When the fourth-order derivative becomes small, the solutions become unstable in the frequency domain. Hence, we should use physical intuition to consider such a limit.

Although some families of exact solutions of the CSHE can be obtained analytically [27], it is clear that this equation can mainly be analyzed only using computer simulations. This has been done in the majority of the papers published so far. For example, Sakaguchi and Brand numerically observed some solitonlike structures [28]. Localized solutions of the quintic CSH equation are similar to those observed in systems described by the previously studied complex Ginzburg-Landau equation. Let us recall that some analytic solutions for the cubic and quintic CGLE are known [29–32]. In the case of the cubic $(1+1)$-D equation, analytic solutions describe all possible bright and dark soliton solutions. In contrast, in the case of the quintic equation, the analytic solutions of the CGLE represent only a small subclass of its soliton solutions. Moreover, the stable soliton solutions are located outside of this subclass [32]. Therefore, from a practical point of view, useful results can only be obtained numerically.

We note that, apart from some exceptions, the CGLE generally has only isolated solutions [32,33], i.e., they are fixed for any particular set of the equation parameters. This property is fundamental for the whole set of localized solutions of the CGLE. The existence of isolated solutions is one of the basic features of dissipative systems in general. The qualitative physical foundations of this property are given in Ref. [34]. Like the CGLE, the CSH equation models dissipative systems, and we expect that it will have this property. Indeed, our numerical simulations support this conjecture.

In this work, we have found a few additional effects that occur in the CSHE model of a passively mode-locked laser. First, we have found that the CSHE has a greater variety of solutions than the CGLE model. Second, composite stationary and moving pulses are generated for a wider range of parameters than is the case with the CGLE. Finally, we have found that three different types of bound soliton states are generated, in contrast to the CGLE where we had only one type.

The rest of the paper is organized as follows. In Sec. II we present the master equation that we are dealing with and discuss the differences between CSHE and CGLE models of a passively mode-locked laser. Section III presents the details of our numerical simulations. Sec. IV shows a variety of examples of composite and moving solitons of the CSHE, and gives comparisons with the corresponding solutions of the CGLE. Various types of double-pulse solutions and their possible applications are discussed in Sec. V. Finally Sec. VI summarizes our main conclusions.

II. MODEL

The CSH equation with the quintic nonlinear term can be written in the form

$$i\psi_t+\zeta\psi_{xx}+\gamma\psi_{xxxx}+\xi|\psi|^2\psi+\chi|\psi|^4\psi=i\delta\psi, \qquad (1)$$

where the four coefficients ζ, γ, ξ, and χ are complex and δ is real. Equation (1) is written in the form we will refer to as the generalized CSH equation. Then the quintic CGLE is a particular case of Eq. (1) with the coefficient γ being set to zero. To be consistent with our previous works, we shall use the same notations as for the case of the CGLE [32], namely, $\zeta=\zeta_1-i\beta$, $\gamma=\gamma_1-i\gamma_2$, $\xi=\xi_1-i\epsilon$ and $\chi=\nu-i\mu$. Assuming anomalous dispersion and a self-focusing nonlinearity, and using a proper normalization, we can always fix the parameters ζ_1 and ξ_1 to have the values $\zeta_1=0.5$ and $\xi_1=1$. The effects of higher-order dispersion have been studied earlier in Refs. [23–26]. In this work, for simplicity, we ignore the higher-order dispersion, i.e., we put $\gamma_1=0$. As a result, Eq. (1) can be written in a simpler form:

$$i\psi_t+\tfrac{1}{2}\psi_{xx}+|\psi|^2\psi+\nu|\psi|^4\psi=i\delta\psi+i\epsilon|\psi|^2\psi+i\mu|\psi|^4\psi+i\beta\psi_{xx}+i\gamma_2\psi_{xxxx}. \qquad (2)$$

Equation (2) has been written in this way so that all nonconservative terms are on the right-hand side. Notations here are the same as for the CGLE [32] with the only additional term being $i\gamma_2\psi_{xxxx}$.

When applied to pulse propagation in a laser system, the interpretation of the variables is the following: t is the propagation distance or the cavity round-trip number (treated as a continuous variable), x is the retarded time in a frame of reference moving with the pulse, the term with ϵ represents nonlinear gain (or 2-photon absorption if negative), and δ the difference between linear gain and loss. The spectral filtering is now represented by two coefficients β and γ_2 instead of just one, as was the case for the CGLE.

Equation (2) describes nonconservative systems and thus does not have any conserved quantities. Instead, we can write a balance equation for the pulse energy, $Q=\int_{-\infty}^{\infty}|\psi|^2dx$. It is

$$\frac{dQ}{dt}=2\int_{-\infty}^{\infty}\left[\delta|\psi|^2-\beta\left|\frac{\partial\psi}{\partial x}\right|^2+\gamma_2\left|\frac{\partial^2\psi}{\partial x^2}\right|^2+\epsilon|\psi|^4+\mu|\psi|^6\right]dx. \qquad (3)$$

For an arbitrary solution, the energy is not conserved and the integral on the right-hand side is nonzero. However, for any stationary solutions, the t derivative is zero. The first three terms on the right-hand side of the above equation determine the spectrally dependent linear losses and they have to be balanced with the nonlinear gain defined by the two subsequent terms. Again, compared with the balance equation for the CGLE [32], we can see that the main difference between the CSH equation and the CGLE lies in its more involved spectral filtering term, which includes the term with γ_2. The latter is important in describing more detailed features of an actual physical problem.

In order for the pulse to be stable in frequency domain, the coefficient γ_2 must be positive. Then β can have either sign, in contrast to the CGLE case where β had to be positive. A positive β gives a spectral response with a single

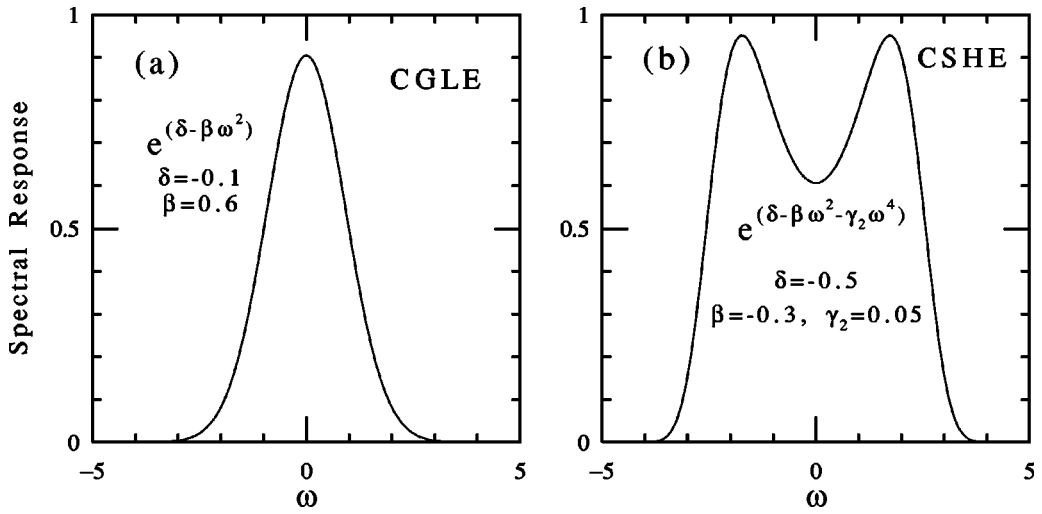

FIG. 1. Spectral filtering $T(\omega)=\exp(\delta-\beta\omega^2-\gamma_2\omega^4)$ in the two models of a laser: (a) CGLE and (b) CSHE. Parameters of the calculation are (a) $\beta=0.6$, $\gamma_2=0$, and $\delta=-0.1$, and (b) $\beta=-0.3$, $\gamma_2=0.05$, and $\delta=-0.5$.

maximum, although the actual shape of the filter is more complicated than in the CGLE model. A negative β gives a spectral response with two distinct maxima. This is the case that will be studied in this work, as it may give some more features of solitons in this model. It is clear that the limit of the CGLE model cannot be reached just by taking $\gamma_2\to 0$, as the pulses will then obviously be unstable. Thus, we have to discuss this issue in more detail.

For clarity, the spectral filtering effect is shown in Fig. 1. It is described by the transfer function $T(\omega)=\exp(\delta-\beta\omega^2-\gamma_2\omega^4)$. The curve in Fig. 1(a) shows the spectral filtering in the case of the CGL equation (with $\gamma_2=0$), and the curve in Fig. 1(b) shows the spectral filtering in the case of the CSHE. The curve on the left is a Gaussian, $\exp(\delta-\beta\omega^2)$, whose amplitude and width are determined by δ and β, respectively. For the CSH equation, the spectral filtering is more complicated and depends on three parameters. This allows us to additionally control the value of the minimum in the spectral dip and the distance between the two maxima in the spectral response. The addition of a third-order derivative on the right-hand side of Eq. (2) would additionally give some asymmetry to the spectral filtering. However, this asymmetry is beyond our interest in this particular work.

The curve in Fig. 1(a) is calculated for the values of the parameters in the CGLE, which were chosen in our previous simulations [35,36], namely, $\beta=0.6$, and $\delta=-0.1$. For calculating the right-hand-side curve, we took $\gamma_2=0.05$, $\beta=-0.3$, and $\delta=-0.5$ in Eq. (1). These latter values of the parameters are chosen in such a way that the total width and the total height of the two spectral responses are not very different. However, as the spectral profiles are different, equivalent solutions in the two cases appear at different values of the cubic gain ϵ.

III. NUMERICAL SIMULATIONS

We have made our simulations using a split-step Fourier method using the fast Fourier Transform for solving the dispersion and filtering parts (x-derivative terms). The method is standard and has been described elsewhere. To find the stationary solutions of Eq. (1) we used the technique of convergence. For a dissipative system, stationary localized solutions are attractors in the functional space, provided they are stable. We are interested only in stable solutions so these attractors are the objects of our study.

Any smooth function that is close enough to an actual solution will be transformed into it during its evolution in t. Hence, to find a solution, we can start with some initial condition close to a soliton profile and wait while it is transformed into a stationary solution. If one or several such solutions do exist for a given set of parameters, almost any smooth localized initial condition will produce a soliton. The technique is similar to what actually happens in a real laser. Any initial state of the system leads to the generation of pulses if the parameters have been chosen correctly. Finding other solutions requires a more careful choice of the initial conditions. However, using our previous experience with the solutions of the CGLE [37], we were able to find a large variety of solutions.

We are also interested in how the solutions change when we change the parameters of the CSHE. This task is easier, since, for any increment in the value of a parameter, we can use the solution at the previous value of the parameter as the new initial condition. If the solution changes continuously when a parameter changes and if it continues to be stable at the new value of the parameter, this technique guarantees a quick convergence to the stationary solution. In the presence of bifurcations this technique is still applicable, but should be used more carefully [9]. In this way we have found families of localized solutions of the CSHE with ϵ as a variable parameter.

The choice of other parameters for the simulation has been dictated by our previous results for the CGL equation [35,36]. These are values that admit the simultaneous existence of the plain soliton pulse (SP), composite pulse (CP), the new composite pulse (NCP), and moving pulse (MP). The only difference between the two models is in the choice of the parameters for the spectral filtering terms. The latter

were chosen as described in the preceding section. More precisely, we shall consider in the rest of the paper the following values for the equation parameters: $\beta=-0.3$, $\gamma_2=0.05$, $\nu=0$, $\mu=-0.1$, $\delta=-0.5$ whereas ϵ is variable. The reason for ϵ being chosen as a variable parameter rather than any other one is that it can be the parameter that controls the stability of solitons in the dissipative system [38].

Of course, the technique described above does not guarantee that we will find all the solutions that exist for a certain set of parameters. For example, the CGLE admits a multiplicity of soliton solutions which can be stable or unstable [39]. No doubt, the same is true for the CSHE. The complete set of solutions can be found with methods such as the shooting technique or equivalent [32,39]. However, our present technique allows us not only to obtain the stationary shapes of the solitons but also to confirm their stability. Moreover, the set of the most robust solutions is usually revealed. As in experiments with real lasers, robust structures are initially generated [13]. Our technique has the advantage of predicting unknown phenomena. In this work, we concentrate on single-pulse localized solutions, as well as a coupled set of two plain solitons. Below, we consider them separately in Secs. IV and V respectively.

IV. COMPOSITE AND MOVING SOLITONS

In this section we present the results for single-pulse generation. The simplest task was to find plain (sechlike profile) solitons. They are not shown here as the result is more or less trivial. Any Gaussian or sech-type initial condition with width less than 1 and amplitude above 1 generally produces a plain pulse for ϵ in the interval $[0.45,1.75]$, especially for the lower values of ϵ. In spite of the double-peak spectra of the filter, these pulses have the usual ''sech-type'' spectra for the whole range of their existence. The spectrum is centered at the center of the system filter.

For values of ϵ higher than 1.4, composite pulses appear profusely. In terms of increasing width, we call them ''composite pulses'' (CP) [32] and ''new composite pulses'' (NCP) [35]. In our simulations, we have found that there are several branches of higher-order localized solutions with increasing width. For simplicity, we call them higher-order ''NCP.'' Numerical results for CP and NCP pulses are shown in Figs. 2 and 3. They both have symmetric amplitude profile and zero velocity. They were produced with sech-type initial conditions with different widths.

Figure 2 shows the result of propagating the initial condition: $\psi(0,x)=2.5\ \mathrm{sech}(x)$. This initial condition converges to a pulse with a CP profile. Similar evolution can be seen if we excite the pulse with another initial condition reasonably close to the actual solution. The convergence is quick with some radiation being emitted during the process. After this transition, the pulse propagates without any further changes. The example presented in Fig. 2 shows that the distance of convergence is $t\approx 5$.

Figure 3 shows another simulation with an initial condition that is also a sech function but is twice as wide, namely, $\psi(0,x)=2.5\ \mathrm{sech}(x/2)$. The solution in this case converges to a pulse with the NCP profile. The width of the pulse is

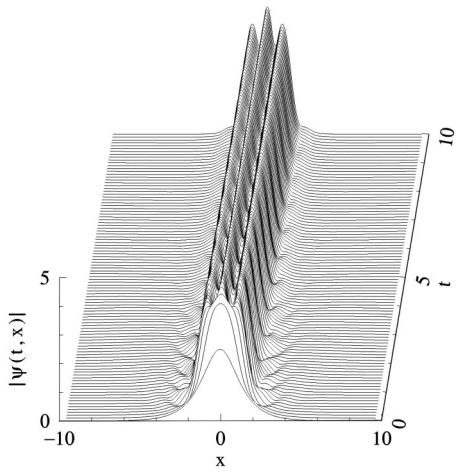

FIG. 2. Convergence of a sech-type initial condition to a CP soliton. Parameters of the simulation are $\beta=-0.3$, $\gamma_2=0.05$, $\epsilon=1.6$, $\nu=0$, $\mu=-0.1$, and $\delta=-0.5$. Here $Q=38.4$.

larger than for the CP and its field amplitude has also more local maxima. Each of these solutions is a symmetric bound state consisiting of two fronts with a sink [40] in the middle.

In general, the convergence to CP and NCP pulses in the case of the CSHE model is faster than in the case of the CGLE model. The reason, as we discussed previously, is the spectral feature of the filter. For the chosen values of parameters β and γ_2, this function is double peaked as we have designed it. As we know from the numerical results for the CGLE equation [41], the CP and NCP pulses have also dual-peak spectra, even when there is a single-peak spectral response of the system. Thus, the dual-peaked spectrum of the system should allow a higher probability of generating CP and NCP pulses. This is, in fact, what we observe in our numerical simulations.

Figure 4 shows the spectra of the CP (dashed line) and NCP (solid line) pulses presented in Figs. 2 and 3. They clearly show the two-peaked structure of these two pulses.

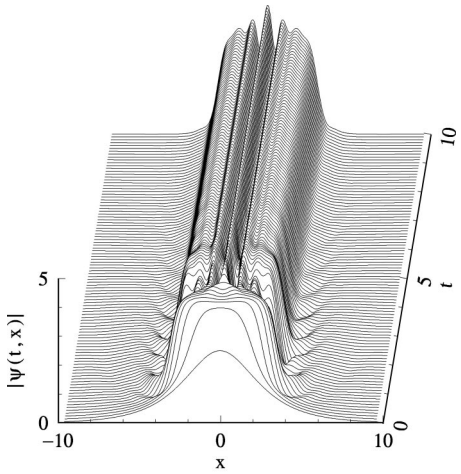

FIG. 3. Convergence of a sech-type initial condition to an NCP soliton. The equation parameters of the simulation are the same as in Fig. 2. Here $Q=74.0$.

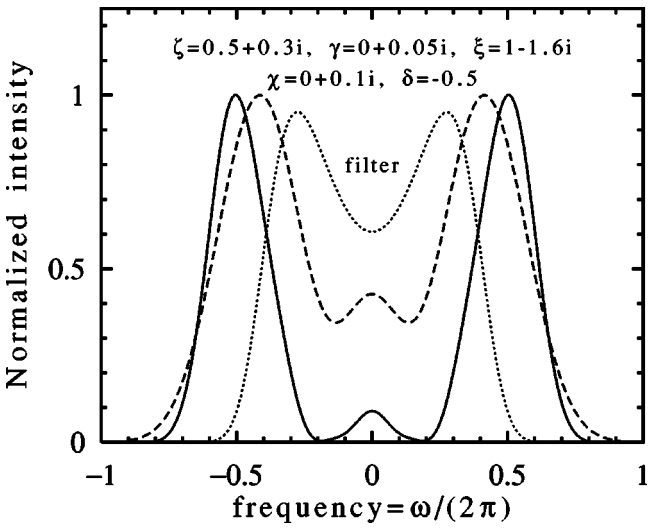

FIG. 4. Spectra of the two pulses [CP (dashed line) and NCP (solid line)] and spectral filtering of the CSHE (dotted line). The parameters are shown in the figure.

This feature is similar to the CP and NCP pulses of the CGL equation [41]. The spectral response of the system (dotted line) is also shown for comparison. The spectral profile of the solution in the nonlinear system does not necessarily have to coincide with the spectral response of the system. However, the similarity facilitates the generation of such pulses.

In addition to the zero-velocity pulses, we have found moving pulses. They are also fixed solutions of the CSHE. For a given set of equation parameters, the shape of the pulse and the velocity are fixed. A solution usually converges to a moving pulse when the initial condition has an asymmetric phase profile. There are many moving pulse solutions. One example of such pulses is shown in Fig. 5. It was excited with the initial condition $\psi(0,x)=2.5\ \mathrm{sech}(x)\exp(ix)$. This initial condition is symmetric in amplitude but has a phase

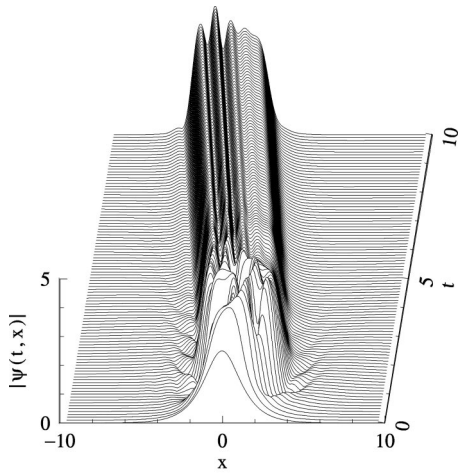

FIG. 5. An example of an asymmetric moving pulse for $\epsilon=1.6$. The pulse energy is $Q=58.9$. This solution is marked in Fig. 9 by a black dot on the middle branch of the MPs (continuous lines).

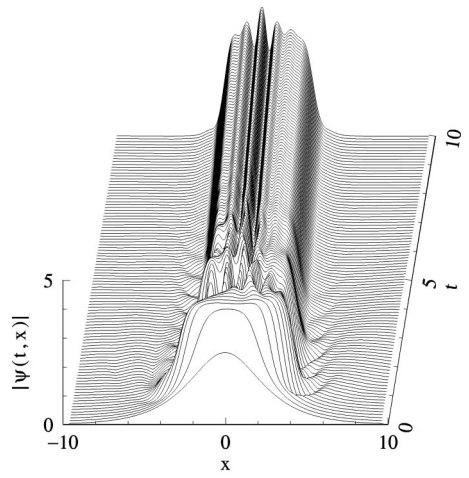

FIG. 6. Another example of an asymmetric moving pulse. Parameter $\epsilon=1.6$. The pulse energy $Q=67.6$. This solution is marked in Fig. 9 by a black dot on the upper branch of the MPs.

asymmetry that corresponds to a certain initial frequency shift, which in our dispersive medium produces a corresponding initial velocity of the pulse. The shape of the resultant moving pulses is asymmetric with unequal shoulders. It can be considered as a bound state of two fronts and a sink. The left-hand-side front is similar to the one for the CP soliton in Fig. 2 and the right-hand-side front is similar to that in the NCP soliton in Fig. 3. This example suggests that a variety of combinations is possible.

Another example of a moving pulse is shown in Fig. 6. It was excited with the wider initial condition $\psi(0,x)=2.5\ \mathrm{sech}(x/2)\exp(i2x)$. The final stationary solution is also a bound state of two fronts but the length of the left shoulder is larger than that in Fig. 5. A large variety of moving pulses with different widths exists. In these two cases, pulses are moving to the left. Due to the symmetry of the problem relative to time, (x) reversal, there are also mirror image solutions with the velocity having the opposite sign.

The spectra of these pulses are also asymmetric. They are shown in Fig. 7. They basically consist of two separated pieces with unequal maxima. When the asymmetry of the spectrum is greater, then the velocity of the pulse is also higher. Stable moving pulses exist for a range of parameters comparable with those for CP and NCP solutions.

So far we have shown how four different soliton solutions are excited. There are many more solutions for the same set of values of the equation parameters. Six cases of soliton profiles, comprising the four treated above, symmetric as well as the asymmetric ones, are shown in Fig. 8. They all have a similar central peak, which corresponds to a sink, and an oscillatory structure around it. The solutions differ in the length of each shoulder around the sink and end with a front at each side. The six soliton solutions shown in this figure are stable solutions at the same values of the equation parameters. Each type of moving pulse has a mirror image solution that moves in the opposite direction. These are not shown in Fig. 8(b).

Composite pulses and moving pulses can be considered as bound states composed of a sink with a front at each side of

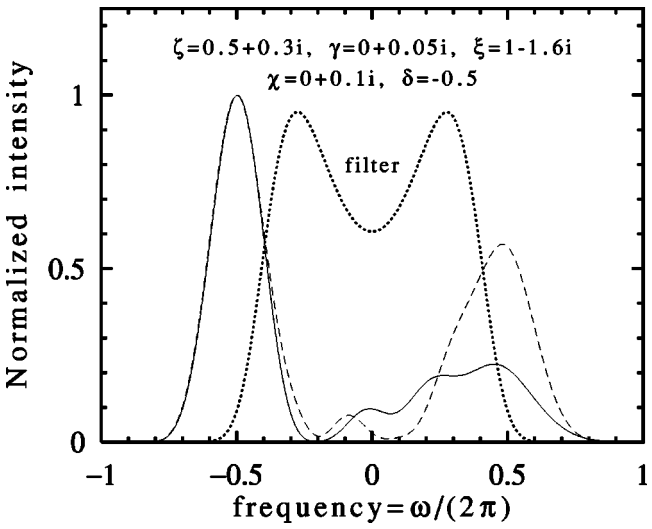

FIG. 7. Spectra of the two moving pulses shown in Figs. 5 (dashed line) and 6 (continuous line), respectively, and spectral filtering of the CSHE (dotted line). The parameters are shown in the figure, and coincide with those in previous figures.

it. Due to the oscillating feature of the sink, the fronts can be located at discrete distances. The variation of these separations creates solitons of different widths. Depending on the location of the two fronts, we can have symmetric and asymmetric pulses.

The variety of soliton solutions obtained for the CSHE model is shown in Fig. 9(a) using the Q-ϵ plane. Soliton branches obtained in the CGLE model are also shown for comparison [Fig. 9(b)]. They have been calculated in our previous work [35]. Comparing the two plots, we can see

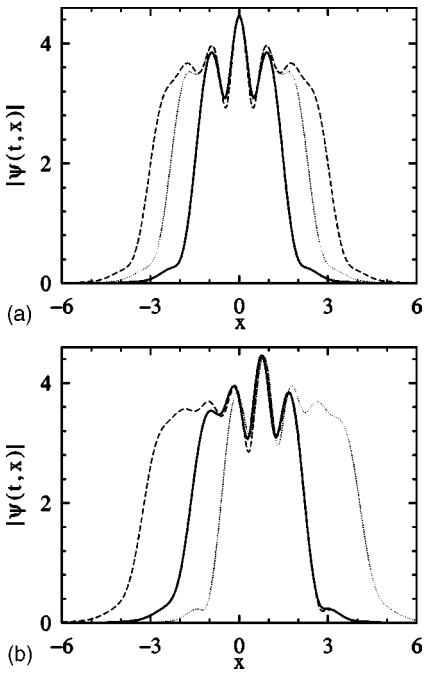

FIG. 8. Various soliton profiles, (a) symmetric and (b) asymmetric (moving solitons). Parameters are the same as in the previous figures.

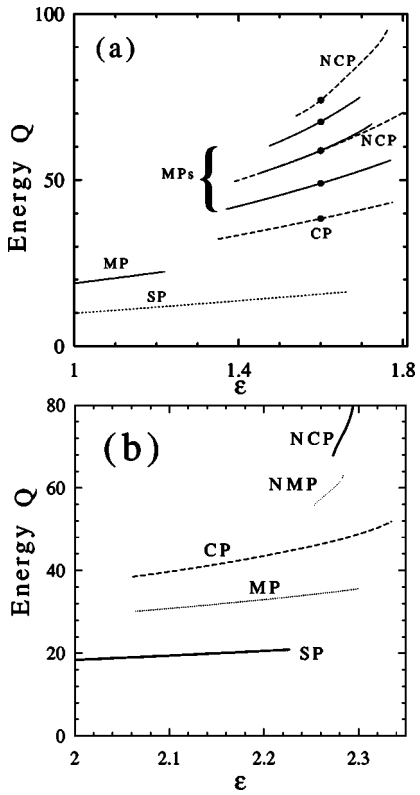

FIG. 9. Various soliton branches in the Q-ϵ plane in the case of the (a) CSH equation and (b) CGL equation (from Ref. [37]). Black dots in (a) correspond to the examples shown in Figs. 8. Parameters of the simulation in the two cases are the same except for the spectral filtering terms and ϵ.

clearly that there are more soliton branches in the CSHE model than in the CGLE model for this set of parameters. We can also notice that the regions of existence and stability for the CP, NCP, and MP pulses are much wider than in the case of the CGL equation.

To see this, we calculated the relative width of the range of existence for each branch of the composite soliton solutions. We denote the lower and upper limits of this range as ϵ_{min} and ϵ_{max}, respectively. Then the relative width for the range of existence is defined as

$$\rho_\epsilon = 2\frac{\epsilon_{max}-\epsilon_{min}}{\epsilon_{max}+\epsilon_{min}}\times 100\%,$$

provided that both ϵ_{min} and ϵ_{max} are positive. For example, in the case of the CSHE model, the range of existence for CP is $\rho_\epsilon = 25\%$ of the parameter ϵ while in the case of CGLE, the range of existence for CP is only around $\rho_\epsilon = 10\%$. Note the different scales and ϵ values along the horizontal axis in Figs. 9(a) and 9(b). This conclusion is similar for all branches of composite and moving solitons. NCP in the CSHE model exists in the range that covers a relative width of $\rho_\epsilon = 12.5\%$. This range for NCP in the case of the CGLE model is only $\rho_\epsilon = 1.3\%$. The conclusion is that the composite and moving solitons are excited more easily in the system with the double-peak spectral features. Convergence to these

solutions is also faster than in the CGLE model. This is also clearly related to the special characteristics of the double-peaked spectral filtering in the CSHE model.

It is worth noting that composite pulses have not been observed in any experiment with a mode-locked laser. This must be related to the fact that they exist only for a narrow range of parameters. Our present numerical results suggest that experimental observations of same can be facilitated if we use double-peaked spectral filtering in the laser system. This can be done, for instance, by using an additional Fabry-Perot filter in the laser cavity. The actual numbers of the filter will depend on the type of laser used in the experiment. For the particular case of the laser used in Ref. [42] a spectral filter with 5 nm of separation between peaks will create pulses of $\approx$100 fs width. The relative depth of the spectral filter in our simulations (minimal transmission in the center versus maximum at the peaks) is $\approx$65%. Our simulations show that the relative range of values of ϵ (ρ_ϵ) where the composite pulses exist further increases when increasing this depth.

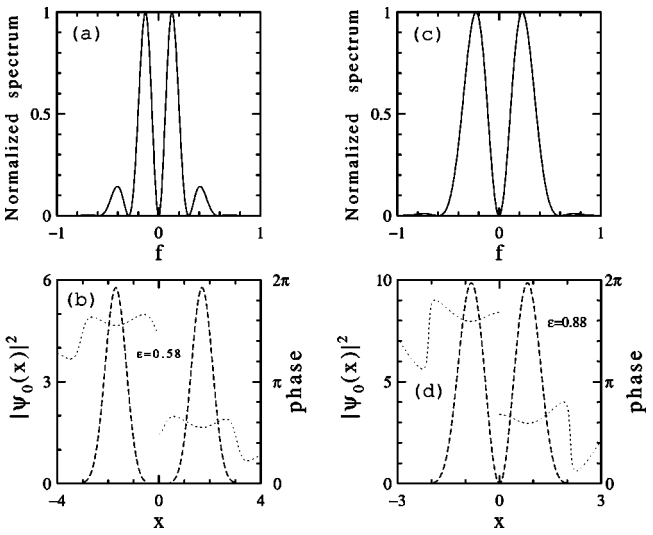

FIG. 10. The (a) spectrum and (b) phase (dotted line) and intensity (dashed line) profiles of a type-I double-pulse solution in the CSHE model at $\epsilon=0.58$. (c) and (d) show the same for the type-II double-pulse solution at $\epsilon=0.88$.

V. DOUBLE-PULSE GENERATION

Several experimental groups have reported double- and multiple-pulse generation from passively mode-locked lasers [14,42–45]. These observations have been made mostly by chance or based on previous numerical simulations. The design of reliable sources of pulse trains with high repetition rates is one of the goals for achieving high-bit-rate information transmission in all-optical lines. Therefore any proposal for achieving two- and multiple-pulse generation with fixed separation between the pulses is an important practical issue.

In our simulations, we have also found that the double-peak structure of the spectral response could facilitate the generation of double-pulse solutions. The reason is that double-pulse solution with a π phase difference between the pulses produces a spectrum with two main equal maxima that could match the spectral response of the system. This indeed occurs in the numerical simulations.

We started our simulations with an initial condition consisting of two single solitons with a small separation between them. This initial condition converges to the two-pulse solution if such a solution exists for the chosen set of parameters. Once one double-pulse solution is obtained, the value of ϵ is changed and this solution is taken as an initial condition in order to find out for which values of ϵ this type of solution remains stable. We used the same set of parameters used in the above simulations, only changing the value of ϵ. We obtained three different types of solutions in this way.

There are two types of double-pulse solutions with approximately π phase difference between the pulses. We denoted them as type-I and type-II solutions. These two solutions mainly differ in the separation between both pulses. They appear at different values of ϵ, i.e., they are not solutions of a given CSHE simultaneously. Moreover, these solutions are separated in ϵ by an interval (0.68–0.78). Switching between these two different types of pulse pairs can be achieved by changing the parameter ϵ across this interval. Such switching will change the pulse separation from one fixed value to another. It is worth mentioning that in addition to the possibility of switching, the stability at the separation distances here must be higher than the stability of spacing related to gain relaxation phenomena [43]. This is due to the general fact that dynamical systems with internal resonances, if used as clocks, are more accurate than systems with relaxation oscillations [46]. In particular, the stability of pulse spacing is higher.

Figure 10(a) shows the spectrum and Fig. 10(b) shows the phase (dotted line) and intensity (dashed line) profiles of the type-I double-pulse solution. As expected, the spectrum of the solution consists of two symmetric strong peaks and two additional sidebands. The type-II solution is shown in Figs. 10(c) and 10(d). This solution has more energy in the two central spectral peaks and very little in the side lobes. All these pulses appear as a result of convergence of the initial conditions to them after a short length.

In addition to the π dephased pair of soliton solutions, there is a solution having a $\pi/2$ phase difference between the two pulses. An example of this type of solution for $\epsilon=1.1$ is shown in Fig. 11. In (a) we show the phase and intensity profiles and in (b) its spectrum. For this solution, the phase profile and the spectrum must be asymmetric [47].

The energy of the double-pulse structure is close to double the energy of a single soliton but they are not identical. The energy Q versus ϵ for the three types of solutions mentioned above is presented in Fig. 12. The dotted line corresponds to the type-I solutions, and the solid line to the type-II solutions. These two curves cover two separate intervals in ϵ and do not appear simultaneously. The dashed curve in this figure corresponds to the solutions with the $\pi/2$ phase difference between the two pulses. Among the two-pulse solutions, this latter solution has a wider range of existence than the type-I and type-II solutions, as can be seen from Fig.

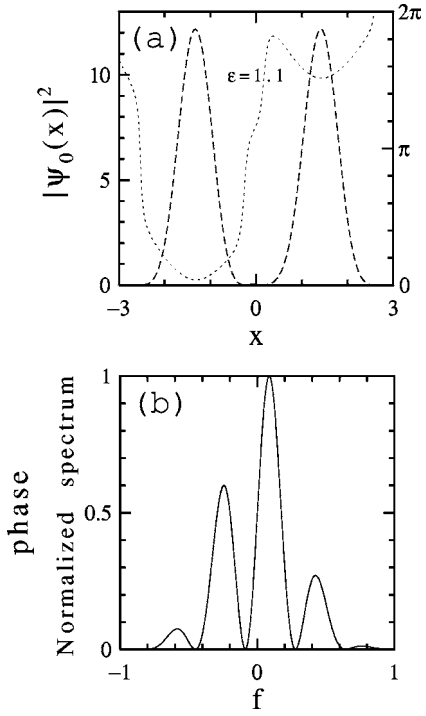

FIG. 11. The (a) intensity and phase profile and (b) spectrum of the double-pulse solutions with $\pi/2$ phase difference between the pulses in the CSHE model.

12. Moreover, it coexists with the type-II solution wherever this latter solution is stable. It also coexists with the type-I solution in a small interval of values of ϵ, namely, in [0.64,0.68]. The solutions labeled π_{I} and $\pi/2$ have almost exactly the energy of two single solitons, while the energy of the π_{II} solutions differs slighlty from that of two single solitons as the pulses are then much closer and so suffer a much stronger interaction that modifies their common tail.

We recall that multiple-pulse generation occurs in the frame of the CGLE laser model as well [48]. However, these

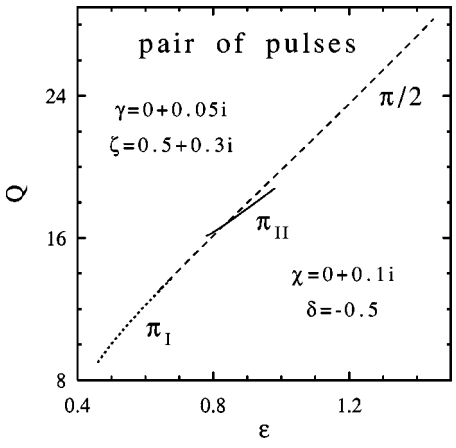

FIG. 12. Energy, Q, versus ϵ for three types of double-pulse solutions. The type-I double-pulse solution with π phase difference between the solitons is shown by the dotted line, whereas the type II is shown by a continuous line. The dashed line represents the double-pulse solutions with a $\pi/2$ phase difference between them.

have different properties. First, stable pairs of solitons in the CGLE model appear only when the phase difference between the pulses is $\pi/2$. In the CSHE model there are at least three stable types of soliton bound states. Second, in the CGLE case, it requires longer propagation distances for the solution to converge to the stationary state than in the CSHE.

The type-II two-pulse solutions (with π phase difference between them) are stationary and stable in the interval of values of ϵ shown in Fig. 12. As we exceed the upper value of ϵ, they are transformed into pulsating solutions. This feature is similar to single-soliton solutions of the CGL equation [9]. In the latter case, the stationary pulses become pulsating ones at the upper edge of their region of stability. Although the two effects are similar, there is an important difference. For a single pulse, the upper edge is close to the point of transition between the existence of pulses and fronts. This is not the case for the two-pulse solutions of the CSHE. Hence the physical reason for the transformation of stationary solutions into pulsating ones should be different. This present transformation is a type of a symmetry breaking instability that results in a phase difference between the two solitons and hence in its motion. When the system parameters are still in the region where the single soliton is stable, the above instability is not destroying the coupled state but causes it to evolve periodically.

The periodic evolution of these pulses is shown in Fig. 13(a). Only one half of the period is shown. In the second half of the period, the pair returns to its original position. The energy of the pair versus z for several periods of evolution is presented in Fig. 13(b) showing the perfect periodicity. As we can see from these figures, the pulses shift each semiperiod of propagation by an amount approximately equal to the width of the solution. This behavior is similar to that of the creeping solutions of the CGLE [9].

The spectrum of this two-pulse solution undergoes periodic changes as well (see Fig. 14). It is slightly asymmetric during the low-velocity part of the evolution due to the fact that the phase difference is not exactly π. After each half period of propagation the larger component swaps to the other side of the solution, as we can see from Fig. 14. The phase shift and separation between the pulses, measured as the distance between the two maxima, also evolves periodically. The periodicity and the values of these changes can be seen from the trajectory shown in Fig. 14(b). The trajectory repeats itself exactly at all successive periods of this motion, forming a closed loop. This proves that the solution is a strictly periodic one. The phase difference is centered around π, but it oscillates, as does the separation between the two pulses.

The last solution presented here belongs to a wide class of pulsating soliton solutions which can take various forms. It is an interesting point that the CSHE has pulsating solutions, as does the CGLE [9]. The whole class of pulsating solutions deserves careful study. However, we cannot focus on this issue here, and leave it for future work. Instead, we have given only one example of a pulsating solution as a proof that they do exist. We stress that these pulsations are not decaying. Pulsating solutions exist on an equal level with

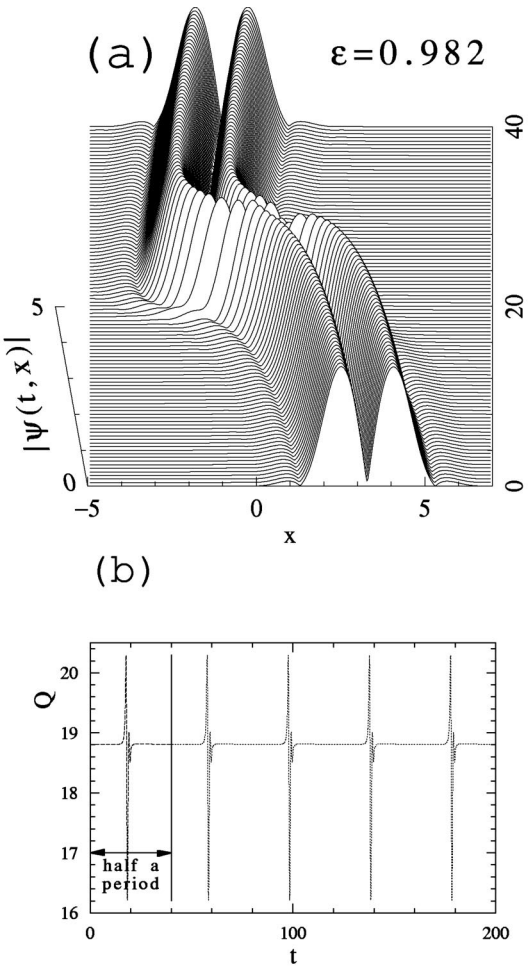

FIG. 13. Periodic evolution of the two-pulse solution with π phase difference between the pulses. (a) Two-pulse profile evolution in half of the period. (b) Energy versus t for 2.5 periods of evolution.

stationary ones, demonstrating the rich dynamics possible in dissipative systems.

We can see from these results that two-pulse generation is also facilitated by using double-peak spectral filters in mode-locked lasers. Several types of two-pulse structures can be generated. Choosing the parameters of the system, the laser can be optimized in order to produce the desired type of pulse pairs or pulse trains with a prescribed separation and phase difference between the pulses. It is remarkable that both phase difference and pulse separation can be controlled by the parameters of the system. The stabilty of the pulse spacing here must be higher than in systems with gain depletion and recovery [43]. Such a laser would be an ideal source of pulses for all-optical high-bit-rate transmission lines.

VI. CONCLUSIONS

In conclusion, we have numerically studied stationary and moving soliton solutions of the quintic complex Swift-Hohenberg equation. We have found that for a specified set of parameters, the system modeled by this equation usually has a larger number of soliton solutions than a system modeled by the complex Ginzburg-Landau equation. This is due to the more complicated spectral response intrinsic to the CSHE model. Our results provide clues for facilitating an experimental observation of composite pulses that have been predicted before, but till now have not been observed. We have also found that the CSHE model of passively mode-locked lasers admits a greater variety of soliton bound states than the CGLE model. In particular, we have numerically found three different types of stable soliton bound states with π or $\pi/2$ phase difference between the solitons. At certain values of the parameters, these solutions may become pulsating. These results suggest the design for an optical pulse train generator with controllable phase shift and pulse separation between the pulses. This would be an ideal source for all-optical high-bit-rate transmission lines. We believe that systematic experimental investigation of two- and multiple-pulse operation of passively mode-locked lasers with special filtering properties is highly desirable.

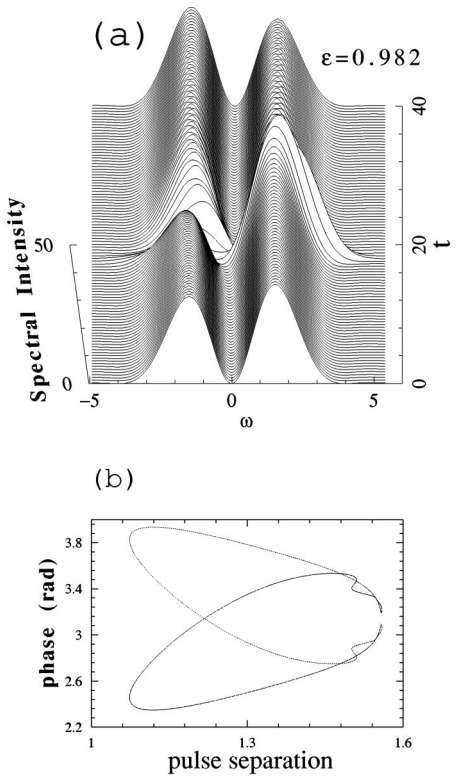

FIG. 14. (a) Evolution of the spectrum of the two-pulse solution with π phase difference between the pulses. (b) Phase shift versus separation between the pulses for this periodic solution.

ACKNOWLEDGMENTS

N.A. acknowledges financial support from the Secretaría de Estado de Educación y Universidades, Spain, Reference No. SAB2000-0197 and from the Australian Research Council. The work of J.M.S.C. was supported by the Dirección General de Enseñanza Superior under Contract No. BFM2000-0806. The authors are grateful to Dr. Adrian Ankiewicz for helpful discussions and for a critical reading of this manuscript.

[1] E.P. Ippen, Appl. Phys. B: Lasers Opt. **58**, 159 (1994).
[2] F.X. Kärtner and U. Keller, Opt. Lett. **20**, 16 (1995).
[3] B.C. Collings, K. Bergman, and W.H. Knox, Opt. Lett. **22**, 1098 (1997).
[4] S. Gray, A.B. Grudinin, W.H. Loh, and D.N. Payne, Opt. Lett. **20**, 189 (1995).
[5] M.T. Asaki, Chung-Po Huang, Dennis Garvey, Jianping Zhou, Henry C. Kapteyn, and Margaret M. Murnane, Opt. Lett. **18**, 977 (1993).
[6] A. Stingl, M. Lenzner, Ch. Spielmann, F. Krausz, and R. Szipöcs, Opt. Lett. **20**, 602 (1995).
[7] D. Coté and H.M. van Driel, Opt. Lett. **23**, 715 (1998).
[8] V.L. Kalashnikov, I.G. Poloyko, V.P. Mikhailov, and D. von der Linde, J. Opt. Soc. Am. B **14**, 2691 (1997).
[9] N. Akhmediev, J.M. Soto-Crespo, and G. Town, Phys. Rev. E **63**, 056602 (2001).
[10] S.R. Bolton and M.R. Acton, Phys. Rev. A **62**, 063803 (2000).
[11] S. Coen, M. Haelterman, Ph. Emplit, L. Delage, L.M. Simohamed, and Reynaud, J. Opt. Soc. Am. B **15**, 2283 (1998).
[12] Q. Xing, L. Chai, W. Zhang, and C. Wang, Opt. Commun. **162**, 71 (1999).
[13] S.T. Cundiff, J.M. Soto-Crespo, and N. Akhmediev, Phys. Rev. Lett. **88**, 073903 (2002).
[14] Ph. Grelu, F. Belhache, F. Gutty, and J.M. Soto-Crespo, Opt. Lett. **27**, 966 (2002).
[15] A.G. Vladimirov, G.V. Khodova, and N.N. Rosanov, Phys. Rev. E **63**, 056607 (2001).
[16] A.K. Komarov and K.P. Komarov, Opt. Commun. **183**, 265 (2000).
[17] V.V. Afanasjev, N.N. Akhmediev, and J.M. Soto-Crespo, Phys. Rev. E **53**, 1931 (1996).
[18] H.A. Haus, J. Appl. Phys. **46**, 3049 (1975).
[19] J.D. Moores, Opt. Commun. **96**, 65 (1993).
[20] J. Lega, J.V. Moloney, and A.C. Newell, Phys. Rev. Lett. **73**, 2978 (1994).
[21] I. Aranson, D. Hochheiser, and J.V. Moloney, Phys. Rev. A **55**, 3173 (1997).
[22] Y. Kuramoto, *Chemical Oscillations, Waves and Turbulence* (Springer, New York, 1984), p. 340.
[23] M. Karlsson and A. Höök, Opt. Commun. **104**, 303 (1994).
[24] N.N. Akhmediev, A.V. Buryak, and M. Karlsson, Opt. Commun. **110**, 540 (1994).
[25] J. Herrmann, V.P. Kalosha, and M. Müller, Opt. Lett. **22**, 236 (1997).
[26] Q. Lin and I. Sorokina, Opt. Commun. **153**, 285 (1998).
[27] A. Ankiewicz, N.N. Akhmediev, and K. Maruno, in Proceedings of ACOFT-27, Darling Harbour, Sydney, 2002 (unpublished), pp. 62–64.
[28] H. Sakaguchi and H.R. Brand, Physica D **117**, 95 (1998).
[29] N.R. Pereira and L. Stenflo, Phys. Fluids **20**, 1733 (1977).
[30] W. van Saarloos and P.C. Hohenberg, Physica D **56**, 303 (1992).
[31] N. Bekki and K. Nozaki, Phys. Lett. **110A**, 133 (1985).
[32] N. Akhmediev and A. Ankiewicz, *Solitons, Nonlinear Pulses and Beams* (Chapman and Hall, London, 1997).
[33] N. Akhmediev, in *Soliton-Driven Photonics*, edited by A. D. Boardman and A. P. Sukhorukov (Kluwer, Dordrecht, 2001), p. 371.
[34] N. Akhmediev and A. Ankiewicz, in *Spatial Solitons*, edited by S. Trillo and W.E. Toruellas (Springer, Berlin, 2001), p. 311.
[35] N.N. Akhmediev and J.M. Soto-Crespo, Proc. SPIE **3666**, 307 (1999).
[36] N.N. Akhmediev and J.M. Soto-Crespo, Technical Report No. SaD10-1/197-199, 1996 (unpublished).
[37] J.M. Soto-Crespo, N.N. Akhmediev, and V.V. Afanasjev, J. Opt. Soc. Am. B **13**, 1439 (1996).
[38] J.M. Soto-Crespo, Nail Akhmediev, and G. Town, Opt. Commun. **199**, 283 (2001).
[39] J.M. Soto-Crespo, N. Akhmediev, and K. Chiang, Phys. Lett. A **291**, 115 (2001).
[40] W. van Saarloos and P.C. Hohenberg, Physica D **56**, 303 (1992).
[41] J.M. Soto-Crespo, V.V. Afanasjev, N.N. Akhmediev, and G.E. Town, Opt. Commun. **130**, 245 (1996).
[42] M.J. Lederer, B. Luther-Davies, H.H. Tan, C. Jagadish, N.N. Akhmediev, and J.M. Soto-Crespo, J. Opt. Soc. Am. B **16**, 895 (1999).
[43] J.N. Kutz, B.C. Collings, K. Bergman, and W.H. Knox, IEEE J. Quantum Electron. **34**, 1749 (1998).
[44] H. Kitano and S. Kinoshita, Opt. Commun. **157**, 128 (1998).
[45] D.Y. Tang, W.S. Man, H.Y. Tam, and P.D. Drummond, Phys. Rev. A **64**, 033814 (2001).
[46] A. Andronov, A. Vitt, and C. Khaikin, *Theory of Oscillators* (Pergamon, Oxford, 1966).
[47] N.N. Akhmediev and A. Ankiewicz, Opt. Lett. **19**, 545 (1994).
[48] N.N. Akhmediev, A. Ankiewicz, and J.M. Soto-Crespo, Phys. Rev. Lett. **79**, 4047 (1997)